Detailed magnetization study of superconducting properties of $YBa_2Cu_3O_{7-x}$ ceramic spheres

2008 J. Phys.: Condens. Matter 20 095222

(http://iopscience.iop.org/0953-8984/20/9/095222)

J. Phys.: Condens. Matter **20** (2008) 095222 (8pp) doi:10.1088/0953-8984/20/9/095222

Detailed magnetization study of superconducting properties of $YBa_2Cu_3O_{7-x}$ ceramic spheres

I L Landau[1,2], **J B Willems**[1] **and J Hulliger**[1]

[1] Department of Chemistry and Biochemistry, University of Berne, Freiestrasse 3, CH-3012 Berne, Switzerland
[2] Kapitza Institute for Physical Problems, 117334 Moscow, Russia

E-mail: landau@iac.unibe.ch

Received 4 December 2007, in final form 25 January 2008
Published 14 February 2008
Online at stacks.iop.org/JPhysCM/20/095222

Abstract

We present a magnetization study of low density $YBa_2Cu_3O_{7-x}$ ceramics carried out in magnetic fields H such that 0.5 Oe $< H <$ 50 kOe. It was demonstrated that superconducting links between grains may be completely suppressed either by a magnetic field $H \sim 100$ Oe (at low temperatures) or by an increase of temperature to above 70 K. This property of the present samples allowed us to evaluate the ratio between the average grain size and the magnetic field penetration depth λ. Furthermore, at temperatures $T > 85$ K, using low field magnetization measurements, we were able to evaluate the temperature dependence of λ, which turned out to be very close to predictions from conventional Ginzburg–Landau theory. Although the present samples consisted of randomly oriented grains, specifics of magnetization measurements allowed for evaluation of $\lambda_{ab}(T)$. Good agreement between our estimation of the grain size and the real sample structure provides evidence for the validity of this analysis of magnetization data. Measurements of the equilibrium magnetization in high magnetic fields were used for evaluation of $H_{c2}(T)$. At temperatures close to T_c, the $H_{c2}(T)$ dependence turned out to be linear, in agreement with Ginzburg–Landau theory. The value of the temperature at which H_{c2} vanishes coincides with the superconducting critical temperature evaluated from low field measurements, which is important evidence of the validity of both approaches to the analysis of magnetization data.

(Some figures in this article are in colour only in the electronic version)

1. Introduction

In this work we present a detailed magnetization study of low density ceramics of $YBa_2Cu_3O_{7-x}$ (Y-123). Data were collected in magnetic fields 0.5 Oe $\leqslant H \leqslant$ 50 kOe. The main attention was paid to the analysis of reversible magnetization, which provides information on equilibrium properties of the superconducting state.

It turned out that superconducting links between the grains are weak and can be suppressed either by a magnetic field as low as 100 Oe (at low temperatures) or by increasing temperature to above $T = 70$ K. As we discuss below, this provides the possibility to study a system of non-interacting grains for gaining information about the relation between the grain size and the magnetic field penetration depth λ.

In magnetic fields $H \sim 1$ Oe, an average grain size of 3–5 μm is too small to capture even a single vortex line, which makes the low field temperature dependence of the sample magnetization $M(T)$ reversible at $T > 70$ K. Analyzing reversible parts of the $M(T)$ curves, the temperature dependence of the magnetic field penetration depth λ can be obtained. Although the present samples consisted of randomly oriented grains, specifics of magnetization measurements allowed for an evaluation of $\lambda_{ab}(T)$.

Magnetization measurements in fields $H \gtrsim 1$ kOe probe completely different physics. In this case, a mixed state is established inside grains and magnetization data provide some of its characteristics. Also here we were interested in reversible magnetization data. As was demonstrated in [1], equilibrium magnetization $M(H, T)$ data allow one to establish the

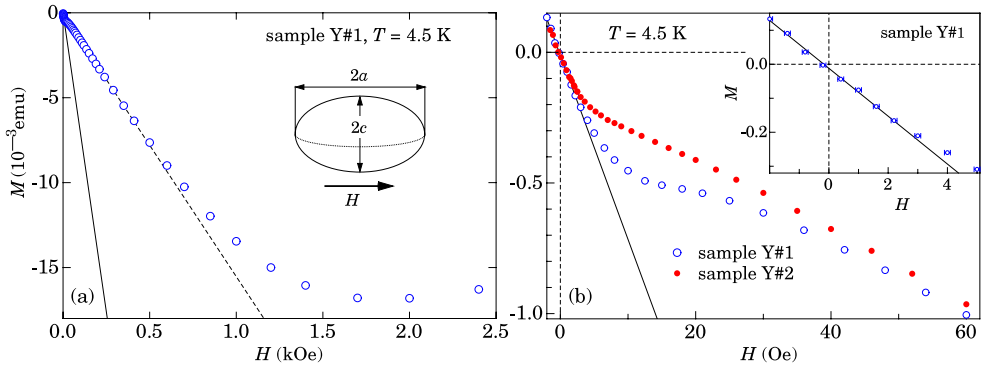

Figure 1. (a) M versus H after zero-field cooling. A magnetic field was applied as illustrated in the inset. The solid and the dashed lines are the best linear fits to the low and the intermediate parts of the $M(H)$ curve (see figures 2 and 3). (b) Low field parts of the $M(H)$ curves. The inset shows results for the sample Y#1 on expanded scales. The straight lines are the best linear fits to data measured in $|H| \leqslant 2$ Oe.

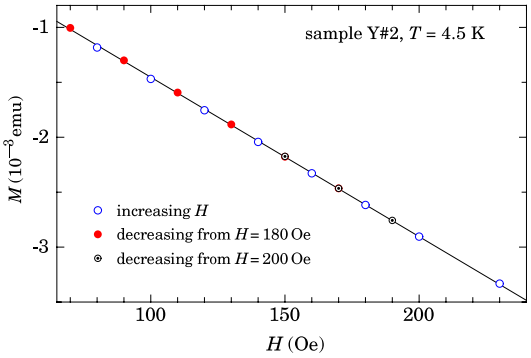

Figure 2. An intermediate part of the $M(H)$ curve for the sample Y#2. The straight line is the best linear fit to data points between 120 and 200 Oe.

temperature dependence of the normalized upper critical field H_{c2}. In this work, we extended measurements up to $T \approx 0.995T_c$ and it was demonstrated that at temperatures close to T_c the $H_{c2}(T)$ dependence is indeed linear in agreement with Ginzburg–Landau theory. Linearity of $H_{c2}(T)$ also allows for a rather accurate evaluation of T_c. We emphasize that T_c determined in such a way is in perfect agreement with the results of low field $M(T)$ measurements. We consider this agreement as additional evidence that the scaling procedure developed in [1] may serve as a reliable tool for the analysis of magnetization data.

2. Experimental details

The samples were made from commercial $YBa_2Cu_3O_{7-x}$ powder (Alfa Aesar). About 0.6 g of powder was suspended in 6 g of 2-butanone by vigorous stirring. Small droplets of this suspension were dropped with a syringe into hemispherical (5 mm diameter) templates made from a flat ZrO_2/BN plate (IEPCO AG). The substrate was initially heated to 250 °C. Rapid evaporation of the solvent lead to flotation of droplets above the surface of the substrate. After several seconds of such flotation, solid spherical samples were formed. These spheres were sintered in a preheated furnace at 700 °C for 30 min. Thereafter, spherical samples were solid enough and could be removed from the substrate and sorted by size. About 30 well formed spheres in the size range of 0.4–1.2 mm were finally sintered in a Al_2O_3 crucible at 940 °C (heating rate 300 °C h^{-1}) in an oxygen atmosphere for 24 h and this was followed by cooling down to room temperature at a rate of 15 °C h^{-1}.

Two samples from this series (Y#1, Y#2) were chosen for measurements. Their shape was very close to an oblate sphere, as schematically illustrated in the inset of figure 1(a). The two samples had practically identical size $2a = (1.2 \pm 0.02)$ mm and $2c = (0.86 \pm 0.03)$ mm with $a/b = (1.4 \pm 0.07)$. While the volumes $V = (0.65 \pm 0.04)$ mm^3 of the samples were almost the same, the masses were slightly different: $m^{(1)} = (2.4 \pm 0.04)$ mg (Y#1) and $m^{(2)} = (2.0 \pm 0.04)$ mg (Y#2). Average densities of the samples were about 0.5 times that for Y-123 single crystals.

All measurements were carried out on a SQUID magnetometer with a 5 T magnet (Quantum Design).

3. Experimental results

The low temperature magnetization curves are shown in figures 1 and 2. In very low fields, M is a linear function of H (see the inset of figure 1(b)). The magnetic moment of a superconducting sample may be written as

$$\frac{4\pi M}{V} = \frac{H}{1 + 4\pi\chi N}, \qquad (1)$$

where N is the demagnetizing factor of a sample and χ is its magnetic susceptibility. In the ideal Meissner state $4\pi\chi = -1$. Substituting in the experimental value of $dM/dH = (7.1 \pm 0.4) \times 10^{-5}$ emu Oe^{-1} and the sample volume, we obtain $N = 0.27$, which is in very good agreement with $N = 0.29$, calculated for an ellipsoid of the corresponding shape [2]. This agreement shows that in fields of some oersteds, superconducting links between grains are strong enough to ensure the coherent superconducting state throughout a sample. In slightly higher fields, however, the deviation of the $M(H)$ curves from linearity indicates breaking of intergrain links.

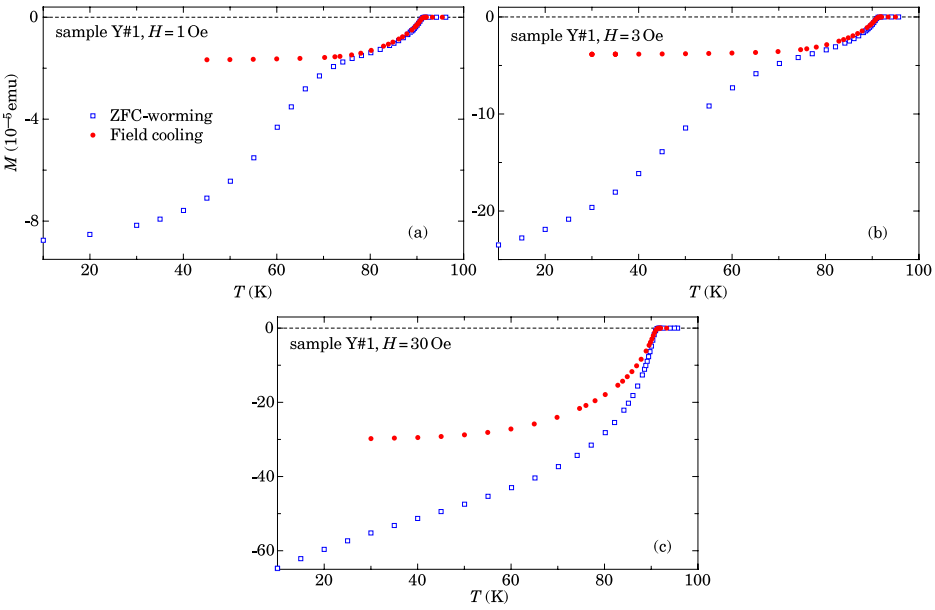

Figure 3. Zero-field-cooled (ZFC) and field-cooled (FC) $M(T)$ curves. (a) $H = 1$ Oe. (b) $H = 3$ Oe. (c) $H = 30$ Oe.

In magnetic fields 50 Oe $< H <$ 250 Oe, the $M(H)$ dependence is again close to a linear function (see figures 1(a) and 2). In addition to exhibiting linearity, the $M(H)$ curve is perfectly reversible (figure 2). This is a clear sign that superconductivity of intergrain links is completely suppressed by a magnetic field, while the field is not yet strong enough to overcome pinning barriers and to penetrate inside grains. The effective formation of the mixed state in grains starts for substantially higher magnetic fields $H > 0.5$ kOe, which is indicated by a saturation of the $M(H)$ curve presented in figure 1(a).

Thus, in magnetic fields between 100 and 200 Oe, our samples can be considered as ensembles of non-interacting grains and their magnetic behavior should be similar to that of a powder. In this magnetic field range, the derivative $\mathrm{d}M/\mathrm{d}H$ may be compared with the total volume of all superconducting grains, $V_S = m/\rho$, where m is the sample mass and ρ is the bulk density of Y-123. Taking experimental values of $\mathrm{d}M/\mathrm{d}H$ and V_S, we get $(1/V_S)(4\pi \mathrm{d}M/\mathrm{d}H) = 0.58 < 1$, i.e., the volume, from which the magnetic field is expelled, is smaller than V_S. This means that the average grain size is comparable with the magnetic field penetration depth λ.

Figure 3 displays temperature dependences of the sample magnetization measured in three different magnetic fields. A steep decline of the sample diamagnetism at $T \approx 60$ K, which may be seen in figure 3(a), corresponds to an effective critical temperature of intergrain links. Another interesting feature is that at temperatures $T \gtrsim 70$ K and $H = 1$ Oe, the sample magnetization is practically reversible, while the reversibility completely disappears for $H = 30$ Oe (figure 3(c)). In the case of $H = 3$ Oe (figure 3(b)), the sample magnetization is close to being reversible although the distance between the two magnetization curves is clearly visible.

The low field magnetic reversibility is not due to vortex motion but rather because grains are too small to capture even a single vortex line. Indeed, if the size of the grain in the direction perpendicular to the field is smaller or of the order of the 'size' of the magnetic flux quantum, $D_0 = \sqrt{\Phi_0/H}$ (Φ_0 is the magnetic flux quantum), no vortices can be created. As an estimate we can use the result of [3] where it was shown that the first vortex is created when the transverse size $D \sim 2D_0$. A similar result was also obtained for very small superconducting spheres [4]. Although [3] and [4] relate to somewhat different geometries, the difference from our case is not expected to be too big.

Considering data presented in figure 3, we may conclude that in $H = 1$ Oe there are practically no grains that can capture a vortex, while the magnetic field of 30 Oe is already strong enough to create the mixed state in a considerable number of grains. The values of D_0 are equal to 4.5, 2.6, and 0.8 μm for magnetic fields of 1, 3, and 30 Oe, respectively. This gives an estimate $r_{\mathrm{eff}} \approx$ 3–5 μm for the biggest grains and $r_{\mathrm{eff}} \gtrsim 1\mu$m for a large number of grains (r_{eff} is an effective grain radius in the direction perpendicular to the magnetic field).

In magnetic fields $H \gtrsim 1$ kOe the mixed state is created in practically all grains and one can see an extended range of reversible magnetization, as illustrated in figure 4, in which the difference $M(T)$–$M(95\,\mathrm{K})$ is plotted. In the following analysis we shall use these equilibrium magnetization data in order to evaluate a temperature dependence of the normalized upper critical field by employing the scaling procedure introduced in [1].

4. Analysis of experimental data

4.1. Superconducting grains in weak magnetic fields

The magnetic moment of a small superconducting sample in the Meissner state depends on the ratio λ/r where $2r$ is the size of the sample in the direction perpendicular to the applied magnetic field. This is why low field magnetization

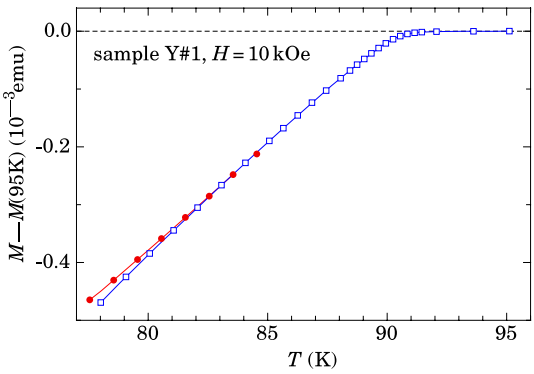

Figure 4. ZFC and FC magnetization curves. The normal state magnetization at $T = 95$ K was subtracted. The solid lines are guides to the eye.

measurements may serve as a valuable tool for evaluation of λ and its temperature dependence. Because the magnetic moment of a single sample with $r \sim \lambda$ is too small to be measured, powder or grain aligned samples were used [5–14]. Here, we apply a similar approach to analyze magnetization data collected on ceramic samples.

For a superconducting sphere the normalized magnetization is [15]

$$\frac{M(\lambda/r)}{M_0} = 1 - 3\frac{\lambda}{r}\coth\frac{r}{\lambda} + 3\frac{\lambda^2}{r^2}, \tag{2}$$

where $M_0 = M(\lambda = 0)$. Because the ratio λ/r enters equation (2) in a rather complex way, the grain size distribution may be important. Usually, this distribution is measured independently and equation (2) is integrated over all grain sizes [9]. In our case, this could not be done reliably. Instead of this, we have analyzed how the grain size distribution may influence magnetization results.

Three different grain size distributions, as shown in figure 5(a), were used. In order to simplify the calculations, the following $n(r)$ were assumed:

$$n(r) = \frac{\pi}{2}\exp\left\{-\frac{(r-1)^2}{2\sigma}\right\} \tag{3}$$

with $\sigma = \sigma_1$ for $r \leqslant 1$ and $\sigma = \sigma_2$ for $r > 1$.

The results of calculations are presented in figure 5(b) on logarithmic scales. Only in the case of the widest grain size distribution ($\sigma_2 = 1$) does the $M(r_0/\lambda)$ curve deviate noticeably from that for a single sphere. Furthermore, the difference between the curves can practically be eliminated by a parallel shift of the curve, which corresponds to some renormalization of r_0 and M_0 (see figure 5(b)). In other words, one can replace integration of equation (2) by introduction of an effective r_0, which is not necessarily equal to the average grain radius. This may lead to some errors in the absolute value of λ, but it is not affecting its temperature dependence.

4.2. Magnetization in low magnetic fields

Equation (2) gives M as a function of λ/r_0, while experiments provide the $M(T)$ curves. In the present analysis, we assume that at temperatures close to T_c, the temperature dependence of λ follows predictions of Ginzburg–Landau theory:

$$\lambda(T) = \lambda_{GL}^{(0)}/\sqrt{1-\tau} \tag{4}$$

with $\tau = T/T_c$.

Substituting equation (4) in equation (2), we obtain

$$\frac{M(T)}{M_0} = 1 - \frac{3\lambda_{GL}^{(0)}}{r_0\sqrt{1-\tau}} \times \left(\coth\frac{r_0\sqrt{1-\tau}}{\lambda_{GL}^{(0)}} - \frac{\lambda_{GL}^{(0)}}{r_0\sqrt{1-\tau}}\right). \tag{5}$$

Equation (5) may straightforwardly be employed for the analysis of experimental $M(T)$ data. There are three adjustable parameters in equation (5), which are not known *a priori*. M_0 changes the vertical scale of the $M(T)$ curve, T_c is the value of T at which the diamagnetic moment of the sample vanishes, and $\lambda_{GL}^{(0)}/r_0$ describes the curvature of the $M(T)$ curve. Because these parameters are related to rather different characteristics of the curve, all of them can be reliably evaluated. We also note some rounding of the $M(T)$ curve at temperatures very close to T_c (see the inset of figure 6). The corresponding data points were not used in the analysis.

As is demonstrated in figure 6, equation (5) provides a rather good approximation to experimental data at temperatures $T \gtrsim 85$ K. This allows for a precise evaluation of

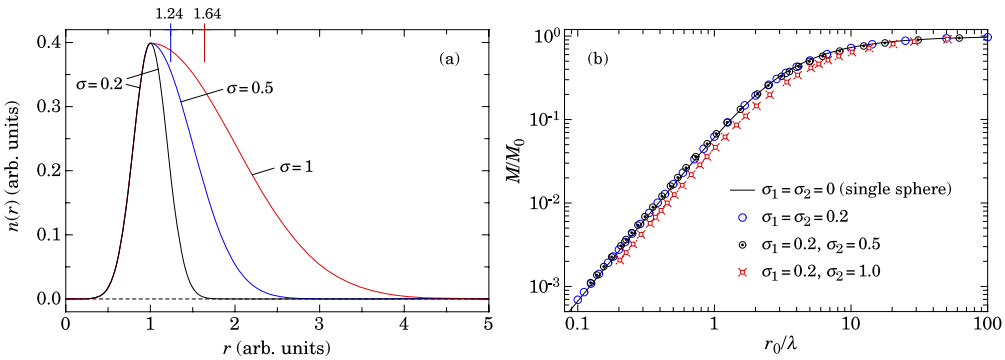

Figure 5. (a) Grain size distributions according to equation (3). The vertical lines indicate average values of radii (r_0) for two asymmetric distributions. (b) The normalized magnetic response M/M_0 as a function of r_0/λ calculated for model distributions described by equation (3) and presented in figure 5(a). The solid line shows the result for a single sphere.

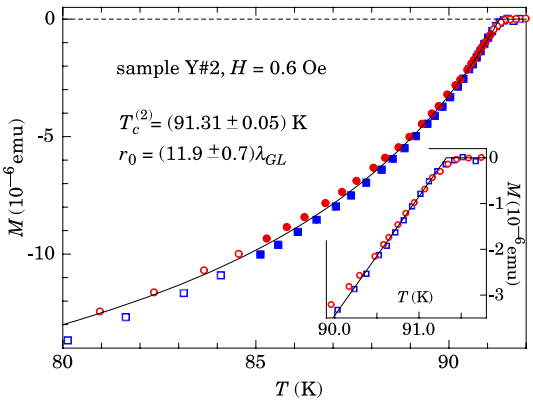

Figure 6. High temperature part of the $M(T)$ curve for the sample Y#2. The solid line is a fit of equation (5) to experimental data. Only data points marked by closed symbols were used for fitting. The resulting values of T_c and r_0 are indicated in the figure. The inset shows $M(T)$ data at temperatures very close to T_c. The straight line is the best linear fit to data measured at 90.5 K $< T <$ 91.2 K. This fit results in $T_c = (91.33 \pm 0.03)$ K.

the superconducting critical temperature for both samples with $T_c^{(1)} = (91.19 \pm 0.08)$ K (Y#1) and $T_c^{(2)} = (91.31 \pm 0.05)$ K (Y#2). Amazingly, the ratios $r_0/\lambda_{GL}^{(0)}$ turned out to be identical for the two samples. Because the samples were prepared under the same conditions, identical grain size distributions are expected. At the same time, very close values of r_0 for both samples obtained as a result of the analysis of magnetization data may be considered as confirmation of the validity of this approach.

According to equation (2), the magnetic moment is inversely proportional to λ^2 if $\lambda(T) > r$. Taking into account that the temperature dependence of λ is expressed by equation (4), we get $M \sim (1 - T/T_c)$. Because λ diverges at $T = T_c$, the condition $\lambda(T) > r$ is always fulfilled in the vicinity of T_c. As may be seen in the inset of figure 6, high temperature data may be very well approximated by a straight line. Linear extrapolation to $M = 0$ gives $T_c^{(2)} = (91.33 \pm 0.03)$ K, which is in excellent agreement with $T_c^{(2)} = (91.31 \pm 0.05)$ K obtained by fitting of experimental data with equation (5) over a much wider temperature range.

4.3. Magnetization in high magnetic fields

Here we use reversible magnetization data collected in magnetic fields 1 kOe $\leqslant H \leqslant$ 50 kOe in order to evaluate the temperature dependence of the normalized upper critical field H_{c2}. A scaling procedure developed in [1] was used for the analysis of experimental data.

The scaling procedure is based on a single assumption that the Ginzburg–Landau parameter κ is temperature independent. In this case, magnetizations measured at different temperatures but in the same normalized fields $H/H_{c2}(T)$ are proportional to $H_{c2}(T)$. According to [1], the magnetizations of a sample at two different temperatures T and T_0 are related by

$$M(H, T_0) = M(h_{c2}H, T)/h_{c2} + c_0(T)H, \qquad (6)$$

where $h_{c2} = H_{c2}(T)/H_{c2}(T_0)$ is the normalized upper critical field and $c_0(T) = \chi_n(T_0) - \chi_n(T)$ (χ_n is the normal state magnetic susceptibility of the sample). It is important to underline that in experiments χ_n includes also a contribution arising from the sample holder, which may be substantial in the case of small samples. While the first term on the right side of equation (6) describes the properties of the mixed state of ideal type II superconductors, the second one is introduced in order to account for all other temperature dependent contributions to the magnetization. By a suitable choice of h_{c2} and $c_0(T)$, individual $M(H)$ curves measured at different temperatures may be merged into a single master curve $M_{\rm eff}(H, T_0)$. In this way the temperature dependence of the normalized upper critical field $h_{c2}(T)$ can be obtained [1].

We measured $M(T)$ for different magnetic fields, as shown in figure 4. $M(T)$ data can easily be converted into $M(H)$ curves. Several such curves are shown in figure 7(a). In the analysis below we use $[M - M(95\ \text{K})]$ instead of M. Because only the difference $[\chi_n(T_0) - \chi_n(T)]$ enters $c_0(T)$, such subtraction does not change the scaling procedure.

Figure 7(b) shows the scaled magnetization curve for the sample Y#1. As may be seen, agreement between the values of $M_{\rm eff}$ calculated from data collected at different temperatures is practically perfect in both cases. The $M_{\rm eff}(H)$ curve represents the equilibrium magnetization curves for $T = 85$ K. While direct measurements may provide such a curve in magnetic

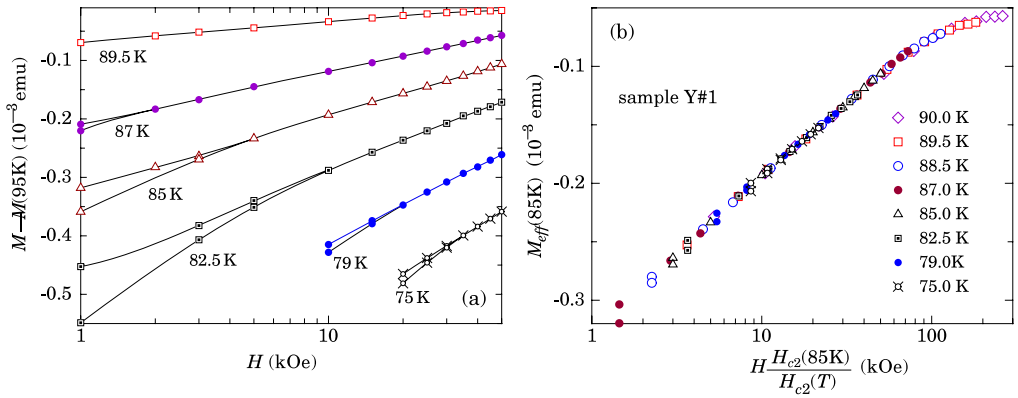

Figure 7. (a) Examples of the $M(H)$ curves for the sample Y#1. The solid lines are guides to the eye. ((b), (c)) $M_{\rm eff}$(85 K) as a function of the normalized field for samples Y#1, Y#2, respectively. Different symbols correspond to $M_{\rm eff}$ calculated from $M(H)$ data collected at different temperatures.

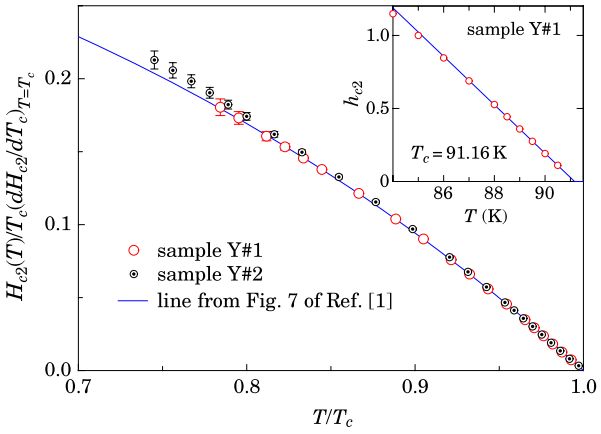

Figure 8. The upper critical field normalized by $T_c(dH_{c2}/dT)_{T=T_c}$ as a function of T/T_c. The solid line is taken from [1]. The inset shows the region near T_c on expanded scales. The solid line in the inset is the best linear fit to data points at $T \geqslant 87$ K. The resulting value of T_c is indicated in the figure.

fields 3 kOe $\leqslant H \leqslant$ 50 kOe, the scaling procedure allows one to establish it in a magnetic field range 10 times wider.

The resulting $h_{c2}(T)$ dependence for one of the samples is shown in the inset of figure 8. At $T \geqslant 87$ K, h_{c2} is a linear function of temperature. This linearity allows for a rather accurate evaluation of T_c by extrapolation of $h_{c2}(T)$ to $h_{c2} = 0$. As a result we obtain $T_c^{(1)} = (91.16 \pm 0.05)$ K. This value is practically the same as $T_c^{(1)} = (91.19 \pm 0.08)$ K evaluated from low field $M(T)$ measurements as shown in figure 6. A similar procedure for the sample Y#2 results in $T_c^{(2)} = (91.26 \pm 0.05)$ K. This value is again in very good agreement with the result of low field measurements (see figure 6).

Because the two samples have slightly different critical temperatures, we plot in figure 8 the normalized upper critical field as a function of T/T_c. For this graph, H_{c2} was normalized by $T_c(dH_{c2}/dT)_{T=T_c}$. As may be seen, the curves for two samples match each other perfectly.

It was established earlier that considering the $H_{c2}(T)$ curves, numerous high T_c superconductors may be divided into two groups with practically identical normalized $H_{c2}(T)$ curves for each of the groups [1, 16–18]. The solid line in figure 8, which is taken from [1], represents such a curve for the larger group. As may be seen in figure 8, the present results for ceramic samples are fully consistent with this curve.

5. Discussion

5.1. Evaluation of T_c

As was demonstrated above, scaling of the $M(H)$ curves allows us to establish temperature dependences of the normalized upper critical field and to evaluate T_c by extrapolation of $h_{c2}(T)$ to $h_{c2} = 0$. The value of T_c can also be evaluated from low field $M(T)$ measurements, as is demonstrated in figure 6. The comparison of these two analyses is presented in table 1.

Table 1. Summary of the evaluation of T_c.

Evaluation method	Sample Y#1	Sample Y#2
T_c from low field $M(T)$ data	91.19 ± 0.08	91.31 ± 0.05
T_c from $h_{c2}(T)$ curves	91.16 ± 0.05	91.26 ± 0.05

We emphasize that T_c was evaluated from two completely different sets of experimental data, which correspond to different physical processes. We argue that the close agreement between the two is convincing evidence that both approaches correctly interpret experimental results. As may be seen in table 1, T_c evaluated from the $h_{c2}(T)$ curves is slightly below the low field estimate. The difference, however, is too small to be speculated on.

5.2. The grain size and the r_0/λ ratio

As was already discussed (sections 3 and 4), magnetization measurement allows for evaluation of λ/r_0 where r_0 is the effective grain radius in the direction perpendicular to the magnetic field. Because in our case the grains have irregular shapes and they are not oriented, reliable estimations of the absolute value of λ are not feasible. We can, however, move in the opposite direction and use literature values of λ in order to evaluate r_0. This is especially interesting because, as we discuss below, magnetization measurements provide three independent ways of evaluation of r_0 and comparison of the resulting values may serve as a consistency check of the theoretical approach. In order to distinguish the different evaluations of r_0, we shall use upper indexes.

The first estimate of the grain size, discussed in section 3, is independent of the magnetic field penetration depth and stems from the fact that in order that the mixed state in separated grains can be created, their size in the direction perpendicular to the magnetic field must be about twice larger than the size of the magnetic flux quantum $D_0 = \sqrt{\Phi_0/H}$ [3, 4]. If grains are too small, no vortices can be created and the sample magnetization $M(T)$ has to be reversible. In the opposite case, $M(T)$ is irreversible. Taking into account that the $M(T)$ curves measured in fields $H \leqslant 3$ Oe are practically reversible, while those in fields $H \gtrsim 30$ Oe are clearly irreversible (see figure 3), we obtain $r_0^{(1)} > 1$ μm (see section 3).

The second estimate was obtained from the fit of the $M(T)$ curve at $T > 85$ K (see figure 6). This gives $r_0 = 11.9\lambda_{GL}^{(0)}$. The value of $\lambda_{GL}^{(0)}$ does not have real physical meaning and it cannot be measured directly; however, it can be calculated from $\lambda(T)$ data in the higher temperature range, in which the temperature dependence of λ follows equation (4). Using results of [20], we obtain $\lambda_{GL}^{(0)} = 0.1$ μm. Considering λ/r_0 in such materials as Y-123, the anisotropy of λ has to be taken into account. In Y-123, the value of λ for currents flowing in the c-direction is $\lambda_c \sim 7\lambda_{ab}$ [19]. At higher temperatures, at which $\lambda_c > r_0$, the situation is simplified by a $1/\lambda^2$ dependence of M (see equation (2)). In this case, the main contribution to M arises from grains with ab-planes approximately perpendicular to H. In this temperature range, averaging leads to $\lambda_{eff} \approx$

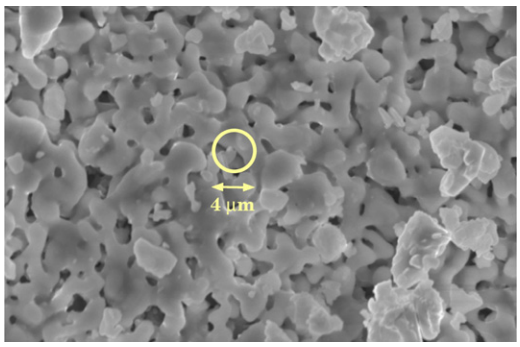

Figure 9. Micrograph of one of the samples. The circle radius corresponds to our estimation of the grain size ($2r_0 = 4$ μm).

Table 2. Summary of r_0 results.

Evaluation method	r_0 (μm)
Onset of irreversibility	$1 < r_0^{(1)} < 3$
$M(T)$ at $T > 85$ K	$r_0^{(2)} \approx 2$
dM/dH at $T = 4.5$ K	$r_0^{(3)} \approx 1.5$

$1.8\lambda_{ab}$. This gives us $r_0^{(2)} \approx 2$ μm in good agreement with the previous estimate.

In fact, there is one more way to evaluate the grain size. As is demonstrated in figure 2, there is a magnetic field range in which the sample magnetization is reversible at low temperatures. In these fields, there are no vortices inside grains and the difference between the ideal Meissner state ($\chi = -1/4\pi$) and the sample magnetization may also be used for evaluation of r_0/λ.

At low temperatures, both λ_c and λ_{ab} are sufficiently small and, according to equation (2), averaging is dependent on the actual value r_0. In the following, we take $r_0 = 2$ μm as was estimated above. Taking $\lambda_c = 7\lambda_{ab}$ and using the commonly accepted value of $\lambda_{ab}(0\ \text{K}) = 0.15$ μm [21], we obtain $\lambda_{eff} \approx 2.7\lambda_{ab}$.

This estimation of the grain size is the only result of this work, which relies on the absolute value of M. In this case, we need to know an effective demagnetizing factor N_{eff} for our sample consisting of a large number of non-interacting grains. For the following estimate we take $N_{eff} = 1/3$. From the slope dM/dH, we obtain $M/M_0 = 0.39$. Substituting this value in equation (3), we get $r_0 = 3.6\lambda_{eff}$. Using the value of λ_{eff} evaluated in the previous paragraph, we obtain $r_0^{(3)} \approx 1.5$ μm.

The resulting values of r_0 are summarized in table 2. All three values are in very good agreement with each other.

Figure 9 shows a micrograph of one of spheres, which was intentionally broken. The circle diameter corresponds to $r_0^{(2)}$, which is the most reliable estimate. Taking into account the approximate character of the consideration, this agreement must be considered as more than satisfactory.

5.3. The temperature dependence of λ

While the absolute values of λ can hardly be evaluated from data collected on ceramic samples, the fact that at $T_c - T \ll T_c$, $\lambda(T)$ follows predictions of the Ginzburg–Landau theory is established quite reliably (see figure 6). As may be seen, $M(T)$ data points follow the theoretical curve at $T > 85$ K. Furthermore, at temperatures very close to T_c, the $M(T)$ dependence is perfectly linear, as is expected from the theory.

Because in this temperature range $\lambda_c \gg \lambda_{ab} \sim r_0$ and $M \sim 1/\lambda^2$, the contribution to the sample magnetization arising from grains with ab-planes oriented along the field is negligibly small and can be disregarded. This means that our results for $\lambda(T)$ are related to λ_{ab}.

The $\lambda_{ab}(T)$ dependence obtained in this work is in agreement with some studies [5–7, 20, 22–25] and in disagreement with data from others [26–28]. We point out that the behavior described by equation (4) was observed for grain aligned samples [6, 7], films [22–24] and single crystals [20, 25]. At the same time, the results of [26–28] provide $\lambda_{ab} \sim 1/(1 - T/T_c)^{1/3}$ instead of equation (4). As far as we are aware this controversy is still unresolved.

6. Conclusion

It was demonstrated that low density ceramic samples of $YBa_2Cu_3O_{7-x}$ may in certain conditions be considered as systems of non-interacting grains. It was also shown that low field magnetization measurements on such samples provide three independent ways of evaluating the grain size (see table 2). All three values are in good agreement with each other and, what is more important, the evaluation of r_0 is in good agreement with the real sample structure (figure 9).

At temperatures close to T_c, low field magnetization data may be very well described assuming that the temperature dependence of λ follows the Ginzburg–Landau theory (figure 6). Although ceramic samples with non-oriented grains were used, it was possible to demonstrate that the above mentioned result is related to λ_{ab}.

The analysis of high field magnetization data allowed us to establish the temperature dependence of the normalized upper critical field. In this work, the upper limit of the temperature range investigated was extended to $T \approx 0.995T_c$ and it was demonstrated that the $H_{c2}(T)$ dependence is a linear function of T at $T \gtrsim 0.95T_c$. This result is in agreement with the Ginzburg–Landau theory. We note that both H_{c2} and λ_{ab} follow the Ginzburg–Landau theory at approximately the same temperatures.

Magnetization measurements presented in this work allowed for evaluation of T_c from two completely different sets of experimental data. It turned out that the two results are in perfect agreement (see table 1).

Acknowledgments

This work was in part supported by the NCCR MaNEP-II of the Swiss National Science Foundation (Project 4). We thank M Bourquin for making ceramic spheres and Professor S Decurtins for enabling the use of a SQUID magnetometer.

References

[1] Landau I L and Ott H R 2002 *Phys. Rev.* B **66** 144506
[2] Osborn J A 1945 *Phys. Rev.* **67** 351
[3] Doria M M and Zebende G F 2002 *Braz. J. Phys.* **32** 690
[4] Baelus B J, Sun D and Peeters F M 2007 *Phys. Rev.* B **75** 174523
[5] Monod P, Dubois B and Odier P 1988 *Physica* C **153–155** 1489
[6] Panagopoulos C, Cooper J R, Athanassopoulou N and Chrosch J 1996 *Phys. Rev.* B **54** R12721
[7] Panagopoulos C, Cooper J R and Xiang T 1998 *Phys. Rev.* B **57** 13422
[8] Panagopoulos C, Cooper J R, Peacock G B, Gameson I, Edwards P P, Schmidbauer W and Hodby J W 1996 *Phys. Rev.* B **53** R2999
[9] Porch A, Cooper J R, Zheng D N, Waldram J R, Campbell A M and Freeman P A 1993 *Physica* C **214** 350
[10] Khasanov R, Eshchenko D G, Karpinski J, Kazakov S M, Zhigadlo N D, Brütsch R, Gavillet D, Di Castro D, Shengelaya A, La Mattina F, Maisuradze A, Baines C and Keller H 2004 *Phys. Rev. Lett.* **93** 157004
[11] Di Castro D, Khasanov R, Grimaldi C, Karpinski J, Kazakov S M, Brütsch R and Keller H 2005 *Phys. Rev.* B **72** 094504
[12] Khasanov R, D Castro D, Belogolovskii M, Paderno Yu, Filippov V, Brütsch R and Keller H 2005 *Phys. Rev.* B **72** 224509
[13] Khasanov R, Häfliger P S, Shitsevalova N, Dukhnenko A, Brütsch R and Keller H 2006 *Phys. Rev. Lett.* **97** 157002
[14] Zuev Y L, Kuznetsova V A, Prozorov R, Vinnette M D, Lobanov M V, Christen D K and Thompson J R 2007 unpublished (Zuev Y L, Kuznetsova V A, Prozorov R, Vinnette M D, Lobanov M V, Christen D K and Thompson J R 2007 *Preprint* cond-mat0707.1905)
[15] Shoenberg D 1940 *Proc. R. Soc.* A **175** 49
[16] Landau I L and Ott H R 2003 *Physica* C **385** 544
[17] Landau I L and Ott H R 2004 *Physica* C **411** 83
[18] Landau I L and Keller H 2007 *Physica* C **458** 38
[19] Zheng D N, Campbell A M, Johnson J D, Cooper J R, Blunt F J, Porch A and Freeman P A 1994 *Phys. Rev.* B **49** 1417
[20] Srikanth H, Zhai Z, Sridhar S, Erb A and Walker E 1998 *Phys. Rev.* B **57** 7986
[21] Khasanov R, Eshchenko D G, Luetkens H, Morenzoni E, Prokscha T, Suter A, Garifianov N, Mali M, Roos J, Conder K and Keller H 2004 *Phys. Rev. Lett.* **92** 057602
[22] Hensen S, Müller G, Rieck C T and Scharnberg K 1997 *Phys. Rev.* B **56** 6237
[23] Andreone A, Cantoni C, Cassinese A, Di Chiara A and Vaglio R 1997 *Phys. Rev.* B **56** 7874
[24] Paget K M, Boyce B R and Lemberger T R 1999 *Phys. Rev.* B **59** 6545
[25] Trunin M R, Zhukov A A, Emel'chenko G A and Naumenko I G 1997 *Pis. Zh. Eksp. Teor. Fiz.* **65** 893 Trunin M R, Zhukov A A, Emel'chenko G A and Naumenko I G 1997 *JETP Lett.* **65** 938
[26] Kamal S, Bonn D A, Goldenfeld N, Hirschfeld P J, Liang R and Hardy W N 1994 *Phys. Rev. Lett.* **73** 1845
[27] Kamal S, Liang R, Hosseini A, Bonn D A and Hardy W N 1998 *Phys. Rev.* B **58** R8933
[28] Anlage S M, Mao J, Booth J C, Wu D H and Peng J L 1996 *Phys. Rev.* B **53** 2792